THE JOURNAL OF BIOLOGICAL CHEMISTRY VOL. 287, NO. 15, pp. 12230–12240, April 6, 2012
Published in the U.S.A.

Neural Crest Deletion of Dlx3 Leads to Major Dentin Defects through Down-regulation of Dspp*[S]

Received for publication, November 28, 2011, and in revised form, January 24, 2012 Published, JBC Papers in Press, February 20, 2012, DOI 10.1074/jbc.M111.326900

Olivier Duverger[‡], Angela Zah[‡], Juliane Isaac[‡], Hong-Wei Sun[§], Anne K. Bartels[‡], Jane B. Lian[¶1], Ariane Berdal[‖], Joonsung Hwang[‡], and Maria I. Morasso[‡2]

From the [‡]Developmental Skin Biology Section and [§]Biodata Mining and Discovery Section, NIAMS, National Institutes of Health, Bethesda, Maryland 20892, the [¶]Departments of Cell Biology and Orthopedic Surgery, University of Massachusetts Medical School, Massachusetts 01655, and the [‖]INSERM, UMRS 872, Universités Paris 5 and 6, Team 5, 75006 Paris, France

Background: Mutations of *DLX3* in humans lead to tooth defects, but normal Dlx3 function in tooth is unknown.
Results: Mice lacking Dlx3 in the dental mesenchyme exhibit major dentin defects, and Dspp is a direct target of Dlx3 in odontoblasts.
Conclusion: Dspp, a major component of dentin matrix, is directly regulated by Dlx3 in odontoblasts.
Significance: Dspp is the first direct target of Dlx3 identified in odontoblasts.

During development, Dlx3 is expressed in ectodermal appendages such as hair and teeth. Thus far, the evidence that Dlx3 plays a crucial role in tooth development comes from reports showing that autosomal dominant mutations in DLX3 result in severe enamel and dentin defects leading to abscesses and infections. However, the normal function of DLX3 in odontogenesis remains unknown. Here, we use a mouse model to demonstrate that the absence of Dlx3 in the neural crest results in major impairment of odontoblast differentiation and dentin production. Mutant mice develop brittle teeth with hypoplastic dentin and molars with an enlarged pulp chamber and underdeveloped roots. Using this mouse model, we found that dentin sialophosphoprotein (Dspp), a major component of the dentin matrix, is strongly down-regulated in odontoblasts lacking Dlx3. Using ChIP-seq, we further demonstrate the direct binding of Dlx3 to the Dspp promoter *in vivo*. Luciferase reporter assays determined that Dlx3 positively regulates Dspp expression. This establishes a regulatory pathway where the transcription factor Dlx3 is essential in dentin formation by directly regulating a crucial matrix protein.

In humans, mutations in the *DLX3* homeodomain transcription factor gene are associated with Tricho-Dento-Osseous (TDO)[3] syndrome, an ectodermal dysplasia characterized by mutation-dependent defects in hair (kinky hair), teeth (enamel hypoplasia and taurodontism), and bone (increased bone density in the cranium and long bones) development (1, 2). Thus far, five mutations in *DLX3* have been associated with TDO syndrome, all of which have an autosomal dominant mode of inheritance. The clinical observations associated with the different mutations in *DLX3* reported so far are associated with highly penetrant tooth defects, and with more variable defects in hair and bone (1–6). Furthermore, dental defects are the most debilitating trait of TDO patients who are highly susceptible to infections and abscesses. The deleterious effects of DLX3 mutations on bone and tooth formation has also been shown in a mouse model overexpressing the 571–574delGGGG DLX3 mutant under the Col1a1 promoter (7, 8).

Although these clinical observations suggest a crucial role for Dlx3 in the development of hair, teeth and bone, the function of Dlx3 in these tissues has not been completely elucidated. Dlx3 knock-out animals die at embryonic day 9.5 (E9.5), due to placental defects (9), making conditional knockouts essential to investigate the role of Dlx3 at later embryonic stages. We previously showed that the conditional ablation of Dlx3 in the epidermis results in a hairless phenotype and the development of an IL17-associated inflammatory response, demonstrating that Dlx3 is required for hair development and skin homeostasis (10, 11). Thus far, conditional deletions of Dlx3 in bone and teeth have not been reported. *Ex vivo* approaches in bone indicate that Osteocalcin (Oc) and Runx2 are directly regulated by Dlx3 (12, 13). Dlx3 target genes in tooth development remain to be identified.

To address the normal function of Dlx3 in tooth development, we used a conditional knock-out approach to delete Dlx3 in the neural crest (NC). In the craniofacial region, Dlx3 is expressed by E9.5 in the post-migratory NC located at the branchial arches (14) and later in several structures derived from this cell population. The dental mesenchyme from which odontoblasts and cementoblasts differentiate to form the dentin and cementum of the tooth, respectively, is derived from the NC (15). During tooth morphogenesis, Dlx3 is initially expressed in the dental epithelium from which ameloblasts differentiate to form enamel, and is later expressed in both the dental epithelium and the dental mesenchyme (16).

All members of the *Dlx* family are expressed in the NC and NC-derived tissues (17). Thus far, *DLX3* is the only member of the *DLX* family in which mutations have been associated with

* This work was supported by the Intramural Research Program of the NIAMS, National Institutes of Health.
[S] This article contains supplemental Figs. S1–S4 and Table S1.
[1] Supported by National Institutes of Health Grant R37 DE012528.
[2] To whom correspondence should be addressed: Developmental Skin Biology Section, NIAMS, NIH, 50 South Drive, Room 1523, Bethesda, MD 20892. Tel.: 301-435-7842; Fax: 301-435-7910; E-mail: morasso@nih.gov.
[3] The abbreviations used are: TDO, tricho-dento-osseous; ChIP-seq, chromatin immunoprecipitation sequencing; NC, neural crest; Dspp, dentin sialophosphoprotein; Oc, Osteocalcin; HERS, Hertwig's Epithelial Root Sheath.

craniofacial defects in humans. In the mouse and human genomes, there are six *Dlx* genes organized into three pairs of inverted and convergently transcribed genes: *Dlx1/2*, *Dlx3/4* and *Dlx5/6* (18, 19). Knocking out *Dlx1*, *Dlx2*, and *Dlx5* results in dental and craniofacial defects (20–22), but early postnatal lethality precluded the analysis of late craniofacial and tooth phenotypes. To date, specific deletion of *Dlx* family members in the NC has not been reported.

Here, we utilized Wnt1-cre mice to delete Dlx3 in the NC (23), and demonstrate that Dlx3 is required for normal odontoblast differentiation and dentin deposition. We further distinguish regulatory pathways where Dlx3 function plays an essential role during tooth development, and identify dentin sialophosphoprotein (Dspp) as a direct target of Dlx3 in odontoblasts. This is the first time a mechanistic link has been established between the transcription factor Dlx3 and the major component of dentin matrix Dspp, both known to be mutated in human disorders associated with dentin abnormalities.

MATERIALS AND METHODS

Mice Breeding and Genotyping—$Dlx3^{LacZ/WT}$ mice and $Dlx3^{F/F}$ mice were generated and genotyped as previously described (10). Wnt1-cre mice (Jax3829) were used to delete Dlx3 in the NC and the activity of the cre recombinase in Wnt1-cre mice was traced by mating with $R26R^{LacZ}$ (Jax3474) or $R26R^{YFP}$ (Jax6148) mice (The Jackson Laboratories, Bar Harbor, ME). Southern blot analysis was used to confirm the deletion of the floxed Dlx3 allele (10). All animal work was approved by the NIAMS Animal Care and Use Committee.

Whole Mount LacZ Staining—Whole mount LacZ staining of Wnt1-cre:$R26R^{LacZ}$ embryos was performed according to Ref. 23. Staining procedure for $Dlx3^{LacZ/WT}$ embryos was described previously (10). Images were acquired using an Olympus SZX9 dissecting microscope (Olympus, Center Valley, PA).

Scanning Electron Microscopy—Samples were fixed overnight at 4 °C in 2% glutaraldehyde, 2% PFA in 0.1 M phosphate buffer, pH 7.4, and dehydrated through a series of 50, 70, 95, and 100% ethanol solutions. They were incubated for 10 min in hexamethyldisilazane, air-dried for 30 min, mounted on aluminum specimen mount stubs covered with conductive carbon adhesive tabs (Electron Microscopy Sciences, Hatfield, PA), sputter-coated with gold and analyzed under a Field Emission Scanning Electron Microscope S4800 (Hitashi, Toronto, Canada) at 10 kV.

High Resolution X-ray and Micro-CT Analysis—Mandibles were fixed in 4% PFA in 1× PBS overnight at 4 °C. For tooth extraction, mandibles were incubated overnight at 55 °C in 2× SSC, 0.2% SDS, 10 mM EDTA, 1 mg/ml proteinase K. High-resolution X-rays were performed using a Faxitron MX-20 and Kodak XTL2 films (5×, 90 s, 40 kV). Micro-CT analysis was performed using a desktop x-ray microfocus CT scanner (Skyscan 1172, Skyscan b.v.b.a., Aartselaar, Belgium). The scanning procedure was completed at 40 kV, at 12 μm per pixel and with a 0.5° rotation step. Reconstruction of raw images into axial cross-sections was performed using NRecon V1.4.0 software (Skyscan). For analysis of the data, measurements and three-dimensional reconstruction, CT-an and CT-vol software were used (Skyscan).

Microarray and Quantitative RT-PCR Analysis—Total RNA was extracted using Trizol® reagent (Invitrogen, Carlsbad, CA) and a tissue homogenizer with disposable plastic probes (OMNI international, Kennsaw, GA). Microarray analysis was performed on three WT and three cKO animals by the NIH NIDDK Genomics Core Facility (24). RNA quality of the samples was tested using bioanalyzer (Agilent Technologies, Santa Clara, CA), and RIN values were above 8.7. 100 ng from each sample was used to amplify the cDNA using NUGEN Applause 3′ Amplification kit, and biotinylated using Encore Biotin module (NUGEN Technologies) according to the manufacturer's instructions. Samples were hybridized with Affymetrix Mouse 430.2 arrays for 18 h (Affymetrix Inc) and processed using Affymetrix 450 Fluidic stations using Affymetrix hybridization, wash and staining solutions. Chips were scanned using Affymetrix GeneChip scanner 3000 running Affymetrix (GeneChip Operating Software) GCOS 1.4 version software. To access the efficiency of cDNA synthesis and labeling Poly-A RNA was spiked to the samples and hybridization controls were added according to the manufacturer's instructions. Wild type samples were averaged and used as a baseline to mutant samples. The significantly affected genes ($p < 0.05$ and fold change ≥ 1.5) were selected based on ANOVA analysis by Partek Pro software (Partek, St. Charles, MO, USA). Quantitative real-time PCR analysis (qPCR) was performed on a MyiQ™ Single Color Real-Time PCR Detection System, using iQ™ Sybr® Green Supermix (Bio-Rad). Primers used: Rs15 (Forward) CTTCCGCAAGTTCACCTACC and (Reverse) GGCTTGTAGGTGATGGAGAA; Dlx3 (Forward) ATTACAGCGCTCCTCAGCAT and (Reverse) CTTCCGGCTCCTCTTTCAC; Dmp1 (Forward) CAGTGAGGATGAGGCAGACA and (Reverse) TCGATCGCTCCTGGTACTCT; Dspp (Forward) AACTCTGTGGCTGTGCCTCT and (Reverse) TATTGACTCGGAGCCATTCC; Mmp20 (Forward) AGATGGCCCTGCATGCGTGG and (Reverse) GAATGGCCCAGGCCCAGAGC; Klk4 (Forward) AAGGCCAGGACTGCTCCCCA and (Reverse) CATCCGGCTGCCAGGCTCTT; Enam (Forward) TCGGAGGGATGTTCTGAAAC and (Reverse) AGGACTTTCAGTGGGTGTGG.

Histology, in Situ Hybridization and Immunohistochemistry—Samples were fixed overnight at 4 °C in 4% paraformaldehyde in 1× PBS, dehydrated, and embedded in paraffin blocks and 10 μm-thick sections were prepared. Radioactive *in situ* hybridization was performed as described by Morasso (25). Immunohistochemical analysis was performed using a blocking solution containing 5% goat serum and 7.5% BlockHen II (Aves Labs, Tigard, OR) in 1× PBS. Signal detection was performed using VECTASTAIN® ABC kit (Vector Laboratories, Burlingame, CA). YFP-expressing samples were prepared for frozen sections using standard procedure. Alexa®-546 anti-rabbit (Invitrogen) was used as a secondary antibody. Riboprobe against Dspp and antibody against Dsp were obtained from Dr. Larry Fisher (26). Rabbit anti-Dlx3 antibody was developed in the laboratory. Rabbit anti-K14 antibody was purchased from Covance (PRB-155P).

Chromatin Immunoprecipitation Sequencing (ChIP-Seq) and qPCR Validation—Primary cells were isolated from mouse mandibles after tissue was minced and digested with trypsin/

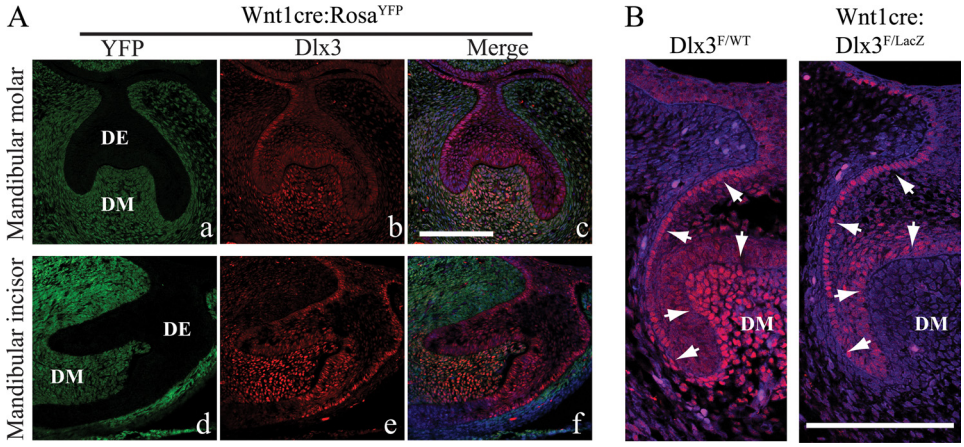

FIGURE 1. **Deletion of Dlx3 in the dental mesenchyme using Wnt1-cre mice.** *A*, Dlx3 expression and activity of the cre recombinase in the developing tooth of Wnt1-cre mice (cap stage). Immunohistochemical analysis using anti-Dlx3 antibody on mandibular molars (*a–c*: coronal section) and mandibular incisors (*d–f*: sagittal section) from Wnt1-cre:R26R^{YFP} at E14.5. *a* and *d*: YFP, *b* and *e*: Dlx3, *c* and *f*: merge. *DM*, dental mesenchyme; *DE*, dental epithelium. *B*, absence of Dlx3 in the dental mesenchyme of the developing molar in Wnt1-cre:Dlx3$^{F/LacZ}$ mice. Immunohistochemical analysis using anti-Dlx3 antibody on mandibular molars from WT and cKO animals at E16.5 (*bell stage*). *White arrowheads* indicate the dental epithelium. Scale bar 50 μm.

collagenase. Cells were grown for 48 h at 37 °C in αMEM medium supplemented with 10% FBS. Chromatin immunoprecipitation was performed according to Ref. 27. Rabbit anti-Dlx3 antibody (Abcam, ab66390) and control rabbit IgG (Abcam, ab46540) were used. Pulled-down chromatin was sequenced using Illumina's Genome Analyzer IIx (GAIIx) after preparation of the samples according to the manufacturer's protocol (Illumina, San Diego, CA). READS of 25 bases were aligned to mouse genome mm9 with Bowtie (28) allowing no more than two mismatches. Statistically significant binding peaks were determined using CisGenome (29) and SICER (30) with default settings and an FDR value of <0.05. For CisGenome, the negative-binomial model was chosen for FDR estimation. Data preparation, data formatting, peak assignment, peak annotations, and the generation of UCSC Genome Browser viewable data files were carried out with in-house developed python scripts. Validation of Dlx3 binding to the Dspp promoter was performed by qPCR on pulled-down chromatin. Primers used: Dspp-prom (Forward) GCAGGGTGACAGAGTCTAAGTGGCT and (Reverse) CCTCGCTCGCCGGTACGTTG.

Dual Luciferase Reporter Assay—The conserved region of the Dspp proximal promoter was cloned into pGL3-basic driving a Firefly luciferase reporter cassette (pGL3-Dspp). Dual-luciferase reporter assay using the Saos2-TetOff osteosarcoma cell line (tetracycline-inducible; Clontech, Mountain View, CA) was performed as previously described (31), using pBi-FlagDlx3 (tetracycline-inducible expression of Dlx3) and pBi-4 (empty vector). Saos2-TetOff cells were co-transfected with one of the pBi constructs, pGL3-Dspp, and the pRL-TK vector (*Renilla* luciferase used for normalization), and grown with (Off) or without (On) doxycycline for 24 h. Relative luciferase activity (firefly/*Renilla*) was measured using the Dual Luciferase Reporter Assay System (Promega, Madison, WI).

Statistical Analysis—All quantitative experiments were performed on at least three control and three mutant animals (Mean ± S.E.). Statistical analyses were performed on Prism 5 statistical software (GraphPad Software Inc., San Diego, CA), using the *t* test with a significance level of 0.05. *: $p < 0.05$; **: $p < 0.01$; ***: $p < 0.001$.

RESULTS

Dlx3 Is Deleted from the Dental Mesenchyme of Wnt1-cre:Dlx3$^{F/LacZ}$ Mice—Whole mount LacZ staining of Dlx3$^{LacZ/WT}$ mice (10) at E11.5 showed that Dlx3 is strongly expressed in the branchial arches where post-migratory NC cells are located (supplemental Fig. S1*Aa*). Cre recombinase activity in Wnt1-cre mice was traced using R26R^{LacZ} mice. At E11.5, Wnt1-cre:R26R^{LacZ} mice expressed LacZ in most of the craniofacial region (supplemental Fig. S1*Ab*). Wnt1-cre mice were mated with Dlx3$^{LacZ/WT}$ mice, and Wnt1-cre:Dlx3$^{LacZ/WT}$ progeny were mated with homozygous Dlx3$^{F/F}$ mice (10). In Wnt1-cre:Dlx3$^{F/LacZ}$ mice, Dlx3 was irreversibly deleted from NC-derived cells. Excision of the Dlx3^{F} allele in Wnt1-cre:Dlx3$^{F/LacZ}$ mice was confirmed by Southern blot at E11.5 (supplemental Fig. S1*B*). qPCR analysis of total RNA isolated from the craniofacial region of Dlx3$^{F/WT}$ (WT) and Wnt1-cre:Dlx3$^{F/LacZ}$ (cKO) mice at E11.5, showed a 10-fold decrease in the level of Dlx3 mRNA expression in cKO mice (supplemental Fig. S1*C*). This illustrates that most of the early Dlx3 expression in the craniofacial region is NC-related and that Dlx3 can be efficiently deleted from the NC using Wnt1-cre mice.

Whereas Dlx3 is expressed in both the dental epithelium and mesenchyme (16), we were expecting a specific deletion of Dlx3 in the dental mesenchyme in Wnt1-cre:Dlx3$^{F/LacZ}$ mice. We examined the distribution of Dlx3 in the developing mandibular molars and incisors at E14.5 in Wnt1cre:R26R^{YFP} mice. At this stage, Dlx3 was expressed in both the dental epithelium and the dental mesenchyme, while the reporter of cre recombinase activity, YFP, was detected specifically in the mesenchyme (Fig. 1*A*). Efficient deletion of Dlx3 in this dental compartment was validated by immunocytochemical analysis on Dlx3$^{F/WT}$ and Wnt1-cre:Dlx3$^{F/LacZ}$ mice (Fig. 1*B*).

Wnt1-cre:Dlx3$^{F/LacZ}$ Mice Exhibit Severe Dentin Hypoplasia and Dysplasia—Even though Dlx3 was deleted in NC-derived bone in Wnt1-cre:Dlx3$^{F/LacZ}$ mice, these mice exhibited mild defects in the structure of craniofacial bones (data not shown). However, major tooth defects could be observed. To characterize the tooth defects in adult Wnt1-cre:Dlx3$^{F/LacZ}$ mice we per-

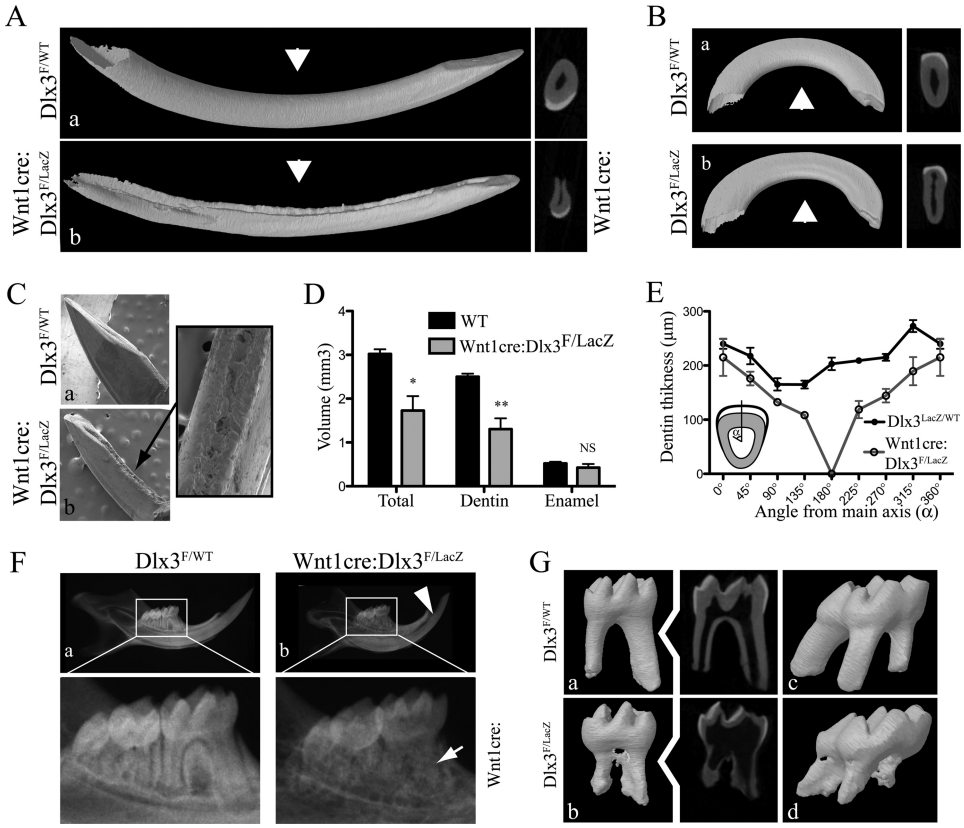

FIGURE 2. **Structural defects in the teeth of adult Wnt1-cre:Dlx3$^{F/LacZ}$ mice.** *A*, micro-CT three-dimensional reconstruction of mandibular incisors at 8 weeks. *Insets* show micro-CT cross section images from the center of the incisors (*white arrowheads*). *B*, same as A for maxillary incisors. *C*, scanning electron microscopy analysis of mandibular incisors at 8 weeks. The *inset* shows the groove in defective incisors. *D*, quantification of tooth volume (total, dentin, enamel) performed on mandibular incisors. *t* test, $n = 3$. *E*, quantification of dentin thickness measured on cross sections of the central part of mandibular incisors (see *A*, *insets*), at different angles from 0 to 360°. *F*, high resolution x-ray of whole mandibles at 8 weeks. *Insets* show a magnification of the molar region. The *white arrowhead* points at the reduced amount of dentin on the lingual side of the mandibular incisor. The *white arrow* points at defects in the structure of the molar roots. *G*, micro-CT three-dimensional reconstruction of first mandibular (*a* and *b*) and maxillary (*c* and *d*) molars at 8 weeks. *Insets* show micro-CT section images of mandibular molars.

formed micro-CT analysis at 8 weeks and found that both mandibular and maxillary incisors exhibited hypoplastic dentin (Fig. 2, *A* and *B*). Dentin defects were more pronounced in mandibular incisors where no dentin formed on the root-analog side of the tooth, leaving an open groove on the lingual side (Fig. 2, *A* and *C*). Significant reduction in the volume and thickness of the dentin was measured in cKO animals (Fig. 2, *D* and *E*). High resolution x-ray of whole mandibles also highlighted incisor defects and revealed that molars exhibited severe root defects (Fig. 2*F*). Micro-CT three-dimensional reconstructions showed that both maxillary and mandibular molars from cKO mice had shorter roots, with a reduction in the thickness of the crown and root dentin, resulting in enlarged pulp chamber and misshapen cusps and root apex (Fig. 2*G*). These data demonstrate that Dlx3 expression in the NC is essential for dentin formation during tooth development.

Dentin is a mineralized matrix produced by odontoblasts which present long cytoplasmic processes that run along dentinal tubules across the whole thickness of the dentin. To further characterize the dentin defects in adult cKO mice, we analyzed the inside surface of mandibular incisors and molars using scanning electron microscopy. In contrast to the regular inner surface of the dentin and the uniform distribution of dentinal tubules observed in control animals, the inner surface of the dentin in cKO mice was rough and the distribution of dentinal tubules was uneven and disorganized (Fig. 3, *A* and *B*). Scanning electron microscopy analysis of incisor cross sections showed that dentinal tubules were visible throughout the whole thickness of the dentin in both WT and cKO animals, but they were more disorganized and thinner in cKO animals (Fig. 3*C*). These observations show that odontoblasts lacking Dlx3 form thinner dentinal tubules and produce dysplastic dentin.

Dlx3 Expression in the Dental Mesenchyme Is Essential for Normal Odontoblast Differentiation and Dentin Formation—The morphogenesis of the molar crown through the bud, cap and bell stages was not visibly altered in cKO mice (Fig. 4*A*), which is consistent with the fact that the overall structure of the molar (number of cusps) appeared unaffected (Fig. 2*G*). After odontoblasts started producing matrix, dentin thickness was reduced and cusp shape was altered in molars from cKO mice (Fig. 4*B*). At P15, the reduced dentin thickness in the crown of molars from cKO mice was more obvious, the predentin/dentin ratio was higher, and the inner surface of the dentin was rough when compared with the control (Fig. 4*C*, *insets 1*).

Radiculogenesis (root development) involves the downgrowth of the dental epithelium at the junction between the inner and outer enamel epithelium. These fuse to form the Hertwig's Epithelial Root Sheath (HERS). Concomitant to

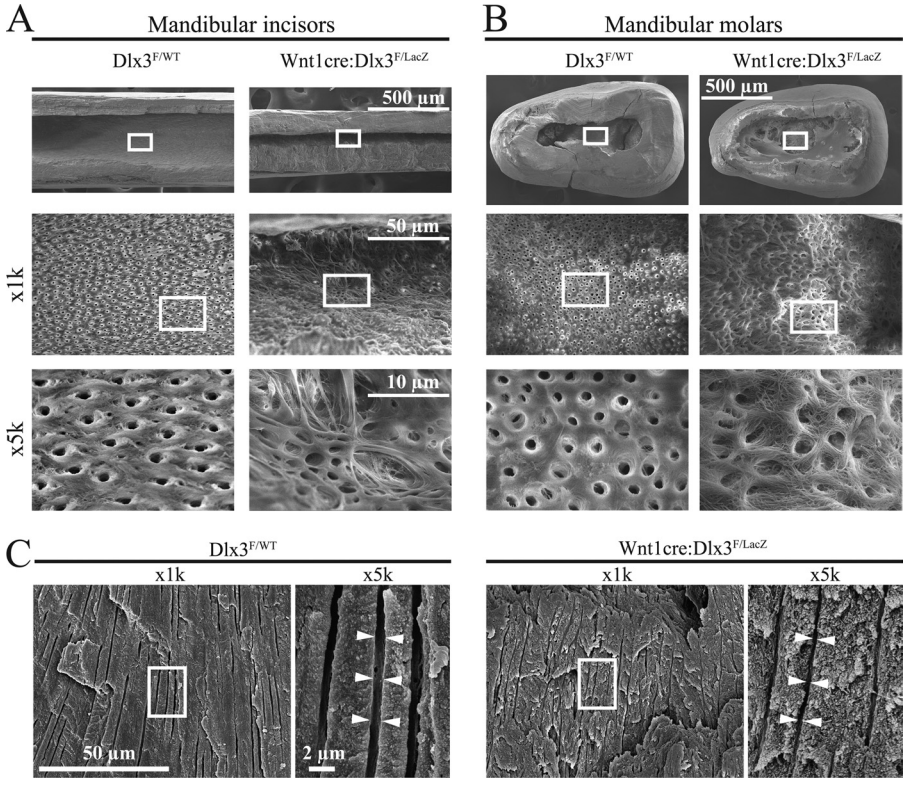

FIGURE 3. **Dentin matrix and dentinal tubule defects in Wnt1-cre:Dlx3$^{F/LacZ}$ mice.** *A*, scanning electron microscopy analysis of the inside surface of dentin in mandibular incisor from cKO and control mice at 8 weeks. The root-analog side of the incisors was removed, and samples were treated with sodium hypochlorite to eliminate soft tissues. *B*, same as *A* for mandibular molar. *C*, scanning electron microscopy of incisor cross sections showing the longitudinal arrangement of dentinal tubules throughout the thickness of the dentin. *White arrowheads* highlight the reduced thickness of dentinal tubules in cKO animals, when compared with WT animals.

the HERS downgrowth, odontoblasts from the dental papilla differentiate and produce dentin on the inner side of the root. On the outer side of the root, cells from the dental follicle differentiate into cementoblasts producing the cementum that establishes the junction between the root and the periodontal ligament. During radiculogenesis, Dlx3 was detected in the HERS and on the dental papilla side of the mesenchyme (odontoblasts and dental pulp), but not in cementoblasts (supplemental Fig. S2).

At the same stage, cKO mice exhibited shorter roots than control mice (Fig. 4*C*). Moreover, at high magnification, the matrix making up the roots in cKO mice did not clearly exhibit the distinct layers visible in control animals: predentin, dentin, and cementum (Fig. 4*C*, *insets 2*). The surface of the root was smoother on the dental follicle side than on the dental papilla side, and the histology of the developing periodontal ligament appeared normal (Fig. 4*C*, *insets 2*), suggesting that Dlx3 is not involved in cementum and periodontal ligament development. Immunohistochemical analysis of HERS cells using K14 antibody revealed that the HERS was normally stained at the base of the developing root, and that the characteristic Epithelial Rests of Malassez (ERM) lining the outer surface of the root were also present in cKO mice (Fig. 4*D*).

The groove observed on the lingual side of adult mandibular incisors in cKO mice, suggests early patterning defects specific to this continuously growing tooth. At E16.5 (bell stage), developing mandibular incisors were smaller in cKO mice, suggesting a delay in the tooth growth of the mutant (Fig. 5*A*). However, the bell shape was not altered, and both the lingual (root-analog) and labial (crown-analog) cervical loops were visible (Fig. 5*A*). By P1, cKO mice showed disrupted alignment of odontoblasts on the labial and lingual sides of mandibular incisors, resulting in a random accumulation of matrix with no distinction between predentin and dentin and the presence of osteodentin evidenced by entrapment of odontoblasts inside the matrix (Fig. 5*B*). Additionally, dentin was almost absent from the most lingual aspect of the root-analog side (Fig. 5*B*, *insets*), which is consistent with the presence of a groove in adult incisors (Fig. 2, *A* and *C*). Longitudinal sections of the mandible at P5 showed that dentin was absent from the lingual side of mandibular incisors along the whole proximal-distal axis of the tooth in cKO mice (Fig. 5*C*, *arrows*). However, the structure of the cervical loop appeared normal at this stage on the lingual side (Fig. 5*C*, *arrowheads*), suggesting that dental epithelium progression is normal. No difference in cell proliferation or apoptosis was found between the incisors of WT and cKO animals at P1 (data not shown).

Taken together, these data reveal that the expression of Dlx3 in the dental mesenchyme is essential for odontoblast differentiation and for dentin deposition and mineralization. Early patterning defects were visible only in the continuously growing mandibular incisor for which the mechanisms leading to the absence of dentin on the lingual side remain to be elucidated.

Ameloblast Differentiation and Enamel Formation Are Not Affected in Wnt1-cre:Dlx3$^{F/LacZ}$ Mice—Although Dlx3 is not deleted from the dental epithelium in Wnt1-cre:Dlx3$^{F/LacZ}$

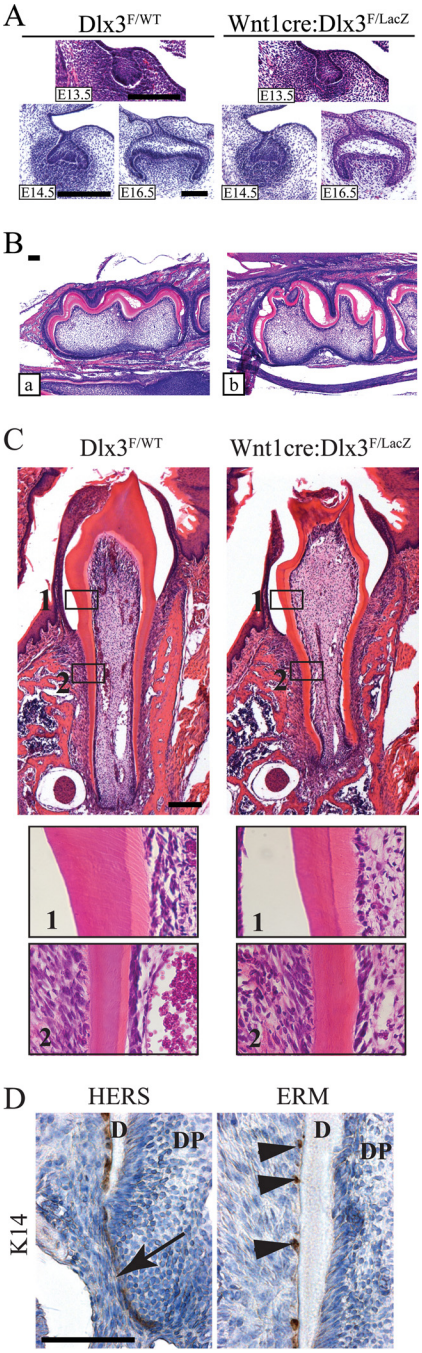

FIGURE 4. **Molar morphogenesis, odontoblast differentiation, dentin deposition, and radiculogenesis in Wnt1-cre:Dlx3$^{F/LacZ}$ mice.** *A*, histology of mandibular molars at E13.5 (bud stage), E14.5 (cap stage), and E16.5 (bell stage) in WT and cKO mice. H&E staining of coronal head sections. *B*, histology of mandibular molars at P5. H&E staining of parasagittal head sections showing longitudinal sections of the molars. *C*, histology of mandibular molars at P15. *Insets 1* and *2* show enlarged views of the crown and root dentin, respectively. *D*, identification of the Hertwig's Epithelial Root Sheath (HERS, *arrow*) and the Epithelial Rests of Malassez (ERM, *arrowheads*) using immunohistochemical analysis of K14 expression on growing roots from cKO mice at P15. Scale bar 100 μm.

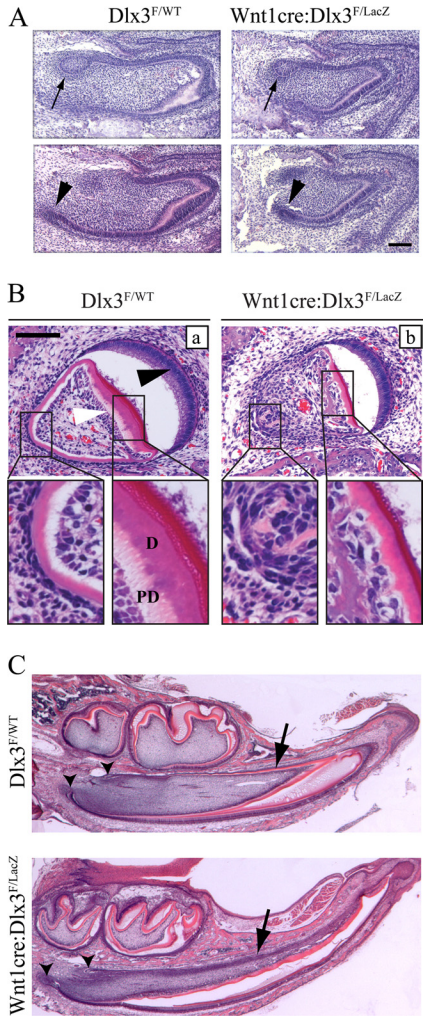

FIGURE 5. **Mandibular incisor morphogenesis, odontoblast differentiation, and dentin deposition in Wnt1-cre:Dlx3$^{F/LacZ}$ mice.** *A*, histology of mandibular incisors at E16.5 (bell stage) in WT and cKO mice. H&E staining of parasagittal head sections. *Arrows* and *arrowheads* indicate the lingual and labial cervical loops, respectively. *B*, histology of mandibular incisors at P5. H&E staining of coronal head sections showing cross sections of the incisors. *Insets* show enlarged views of the lingual and labial sides of the developing teeth. *White arrowhead* indicates odontoblasts, and *black arrowhead* indicates ameloblasts. *PD*, predentin; *D*, dentin. *C*, parasagittal section of mandibles at P5 showing the absence of dentin on the root-analog side of the tooth, throughout the proximal-distal axis of the mandibular incisor in cKO mice (*arrows*). *Arrowheads* indicate the lingual and labial sides of the cervical loop.

mice, the changes in the composition of the dentin matrix in Wnt1-cre:Dlx3$^{F/LacZ}$ mice could indirectly affect the dental epithelium (32). At P5, Dlx3 was detected in the ameloblasts of cKO mice in which it was deleted from the dental pulp and odontoblasts (supplemental Fig. S3*A*). The histology of differentiated ameloblasts at P15 appeared unaffected in cKO animals (supplemental Fig. S3*B*). Consistently, the structure of the enamel matrix deposited by the ameloblasts also appeared normal: the respective morphology of external aprismatic (eae), external prismatic (epe), and internal prismatic (ipe) enamel was not affected, and prism decussation (where bundles of rods cross the enamel-dentine junction to the outer enamel surface) was not altered (supplemental Fig. S3*B*). Scanning electron microscopy analysis of mandibular incisor sections at 8 weeks showed that enamel exhibited a homogenous thickness and a smooth surface, and the structure of the enamel prisms appeared normal in cKO mice (supplemental Fig. S3*C*). The enamel surface of first mandibular molars also appeared normal (supplemental Fig. S3*D*). These data prove that the absence of Dlx3 from the dental mesenchyme does not have any indirect effect on ameloblast differentiation and enamel formation.

A

Gene Symbol	RefSeq Transcript ID	p-value	Fold-Change
Dspp	NM_010080	0.00115	-7.34
Dlx3	NM_010055	2.41E-06	-7.30
Mmp20	NM_013903	0.00437	-4.03
Klk4	NM_019928	0.00178	-2.31
Enam	NM_017468	0.03613	-2.14

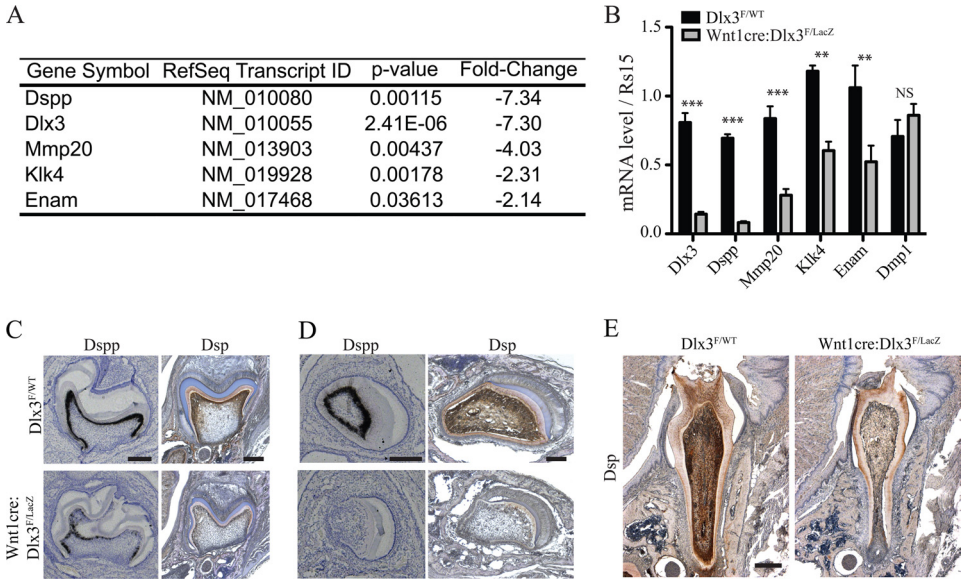

FIGURE 6. **Alteration of gene expression in the mandible of Wnt1-cre:Dlx3$^{F/LacZ}$ mice.** *A*, tooth markers affected by the absence of Dlx3 from NC-derived cells in the mandible, as identified by microarray analysis of total mRNA from mandibles at P0 (cKO *versus* WT). *B*, qPCR validation of microarray analysis. *t* test, $n = 4$. *C*, *in situ* hybridization of Dspp mRNA expression and immunohistochemical analysis of Dsp protein expression in mandibular molars at P5. *D*, same as in C for mandibular incisors. *E*, immunohistochemical analysis of Dsp protein expression in first mandibular molars at P15. Scale bar 100 μm.

Dspp Is Strongly Down-regulated in the Mandible of Wnt1-cre:Dlx3$^{F/LacZ}$ Mice—The phenotypical defects observed on the dentin of Wnt1-cre:Dlx3$^{F/LacZ}$ mice after birth (Figs. 4 and 5), suggest a role for Dlx3 in early odontoblast differentiation. To identify early and direct targets of Dlx3 in this process, and to avoid analyzing late effects that could be indirect and secondary to the absence of Dlx3, total RNA was extracted from mandibles dissected from WT and cKO mice at P0 and used for microarray analysis (Fig. 6*A* and supplemental Table S1) and qPCR validation (Fig. 6*B*). Even though mandibles contain a mixed population of NC-derived mesenchymal cells (bone and dental mesenchyme) and epithelial dental cells, this approach allows the identification of tooth markers affected by the absence of Dlx3 in the dental mesenchyme. Dentin sialophosphoprotein (Dspp) was the most highly down-regulated gene. Processing of the Dspp precursor protein gives rise to dentin sialoprotein (Dsp), a more recently discovered dentin glycoprotein (Dgp) and dentin phosphoprotein (Dpp), the latter being essential for dentin mineralization (33–35). The expression of Dmp1, another major dentin component, was not affected (Fig. 6*B*). Significant down-regulation was also observed for Enamelin (Enam), as well as Matrix Metalloproteinase 20 (Mmp20) and Kallikrein 4 (Klk4), markers known for their essential role in enamel formation and maturation (36–38), respectively. Mmp20 and Klk4 are also expressed in the dental mesenchyme (39). The list of genes detected in the microarray analysis is provided in supplemental Table S1.

Autosomal dominant mutations in the *DSPP* gene in humans lead to Dentinogenesis Imperfecta, characterized by dentin defects and root dysmorphologies (33), and Dspp knock-out mice exhibit enlarged pulp chamber, increased width of the predentin zone, and defects in dentin mineralization (34). The similarity between the phenotypes of Dspp$^{-/-}$ mice and Wnt1-cre:Dlx3$^{F/LacZ}$ mice, together with the strong down-regulation in the expression of Dspp in the mandible of Wnt1-cre:Dlx3$^{F/LacZ}$ mice, prompted us to further investigate this decrease at the histological level. The amount of both Dspp mRNA and Dsp protein, were strongly decreased in the odontoblasts of all teeth (Fig. 6, *C* and *D*). During radiculogenesis at P15, Dsp expression was strongly reduced in the first molar, in both the crown and the root (Fig. 6*E*). These observations suggest that Dspp is a transcriptional target of a Dlx3-regulated pathway in tooth development.

Dspp Is Directly Regulated by Dlx3—To identify direct targets of Dlx3 *in vivo*, we performed a chromatin immunoprecipitation sequencing (ChIP-Seq) assay on primary cells isolated from mandibles at P0. Primary cultures from mandibles at P0 contain a mix of NC-derived mesenchymal cells and epithelial dental cells (supplemental Fig. S4*A*). After 2 days in culture, we verified the expression of Dlx3 in those cells by RT-PCR (supplemental Fig. S4*B*). The ChIP assay was performed using anti-Dlx3 antibody and IgG control, and the pulled-down chromatin was sequenced using Illumina's GAIIx and aligned to the mouse genome. As different peak-calling programs may generate varying results but should be consistent with very significant peaks (40), we used both CisGenome (29) and SICER (30) for detecting significant peaks. Both programs identified hundreds of chromosome regions (peaks) that were pulled down with the anti-Dlx3 antibody. Among these, only a small minority of peaks were in proximal promoter regions with highly conserved sequences among vertebrates. A significant Dlx3 peak was identified in the promoter region of Dspp (Fig. 7*A*), with tags (normalized to per million total READS) of 195 and 198 for CisGenome and SICER, respectively. No peaks were detected for the IgG control sample in the same region (Fig. 7*A*). Using this approach, Dspp was the only gene that was identified in the ChIP-seq analysis and also affected in the microarray. This sequence is in the proximal promoter of *Dspp*, spanning from 104599367 to 104599857 on Chr5 for a total of 491 bases located in a highly conserved portion of the promoter and cov-

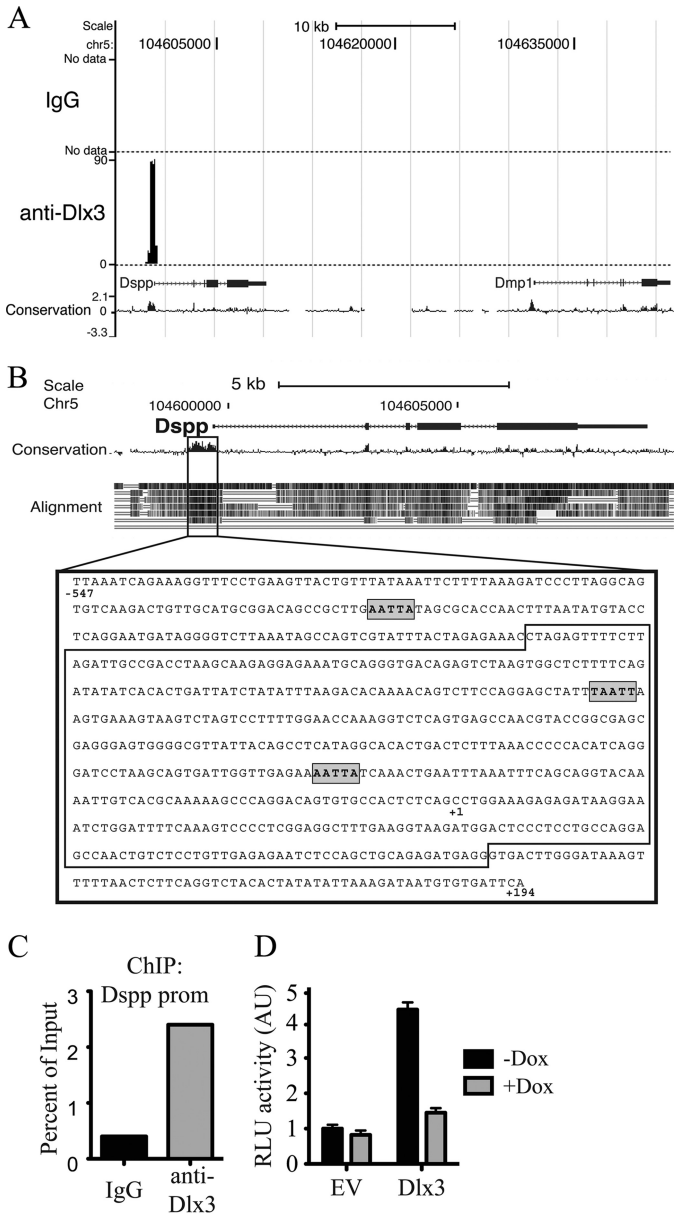

FIGURE 7. **Regulation of Dspp expression by Dlx3.** *A*, UCSC Genome Browser view of Dlx3 binding in Dspp and Dmp1 loci, as determined by ChIP-Seq analysis. Chromatin from primary mandibular cells was immunoprecipitated using anti-Dlx3 antibody and control IgG. Pulled-down chromatin was sequenced using Illumina's GAIIx and aligned to the mouse genome. *Upper* and *lower panels* are for control IgG and anti-Dlx3, respectively. Peak scale shown is for tags normalized to per million total READS. *B*, mouse Dspp locus showing a highly conserved region in the Dspp proximal promoter of several vertebrates. From *top to bottom*, alignment with: rat, human, orangutan, dog, horse, opossum, chicken. Sequence of the conserved region of the Dspp promoter including three potential Dlx3 binding sites (TAATT). The *boxed region* highlights the sequence of the Dlx3 binding peak. +1, transcription start site. *C*, validation of the binding of Dlx3 to the Dspp promoter by qPCR performed on immunoprecipitated chromatin. *D*, dual-luciferase reporter assay using pGL3-Dspp and pRL-TK, with pBi-4 (EV: empty vector) or pBi-FlagDlx3 (Dox-dependant Dlx3 expression), in Saos2-TetOFF cells. −*Dox*, expression of transgene; +*Dox*, repression of transgene expression.

ers two of three Dlx3 consensus binding sites (41) present in this region (Fig. 7*B*). The middle of the peak sequence is 118 bases upstream of the transcript start site of Dspp. The binding of Dlx3 to the Dspp promoter was validated by qPCR using primers located in the conserved region of the Dspp proximal promoter (Fig. 7*C*). The promoter region of the *Dmp1* gene, located right downstream of the *Dspp* locus on chr5, did not show any Dlx3 peak (Fig. 7*A*). This result is consistent with the observation that Dmp1 expression is not affected in Wnt1-cre:$Dlx3^{F/LacZ}$ mice and further supports the specificity of the binding of Dlx3 to the Dspp promoter.

To confirm that Dlx3 positively regulates Dspp expression, the Dspp proximal promoter was cloned into a luciferase reporter plasmid (pGL3-Dspp). A dual luciferase assay was performed using the Saos2-TetOFF osteosarcoma cell line, that has successfully been used to characterize Dlx3 transcriptional activity (31, 42). Co-transfection of Saos2-TetOff cells with pBi-FlagDlx3 and pGL3-Dspp resulted in luciferase activity that was over four times higher than with the empty pBi-4 vector (Fig. 7*D*). The addition of doxycycline to the culture medium, resulting in the shut down of Dlx3 expression, reduced the luciferase activity to basal levels (Fig. 7*D*), confirming that the increased luciferase activity correlates with Dlx3 expression. Taken together, these data reveal that Dlx3 binds to the Dspp proximal promoter *in vivo* and positively regulates its transcription.

DISCUSSION

Even though mutations in *DLX3* have been linked to TDO syndrome (1), the normal function of Dlx3 in tooth development remains unknown. In the present study, by deleting Dlx3 in the dental mesenchyme, we show that Dlx3 is essential for odontoblast differentiation and dentin deposition. We further identify Dspp as a major and direct target of Dlx3 in odontoblasts. This mechanistic link between Dlx3 and Dspp is further supported by the phenotypic similarities observed between $Dspp^{-/-}$ and Wnt1-cre:$Dlx3^{F/LacZ}$ mice. Indeed, Dspp knockout mice exhibit enlarged pulp chamber, widened predentin and defective dentin mineralization (34). Moreover, *DSPP* mutations in humans lead to Dentinogenesis Imperfecta (33).

We previously showed that Dlx3 directly regulates Hoxc13 and several hair keratins in the hair follicle (10), as well as Oc and Runx2 during *in vitro* osteoblast differentiation (12, 13). Our present study identifies Dspp as the first direct target of Dlx3 in odontoblasts. Dspp is produced as a precursor that is cleaved into Dpp, Dgp, and Dsp. Through its high affinity for Ca^{2+} and its ability to bind to collagen fibers, Dpp plays a crucial role in the nucleation and growth of hydroxyapatite crystals during dentin mineralization. Genomic analysis has identified potential enhancer and repressor domains in the Dspp promoter (43, 44). Dspp expression has also been shown to be responsive to BMP-2 signaling, through a regulatory pathway involving the transcription factor NF-Y (45). A more recent finding delineated the BMP2-responsive region within the Dspp proximal promoter and identified five conserved homeodomain elements, two of which are essential for *in vitro* activation by Dlx5 and Msx2 (46). Analysis of the conserved proximal promoter of Dspp led us to the identification of three canonical Dlx3 binding motifs. We previously determined a similar binding affinity for Dlx3 and Msx1 to TAATT sequences *in vitro*, suggesting possible overlap in the target genes for these two homeoproteins (41). Furthermore, there is a complex interplay between the transcriptional activities of Dlx3, Dlx5, and Msx2 on the Oc promoter during osteoblast

differentiation *in vitro* (12), which suggests some overlap in regulatory function. Here we demonstrate for the first time in an *in vivo* model that the transcriptional activation of Dspp is Dlx3-dependent through direct binding of Dlx3 to the Dspp proximal promoter. Still to be determined are the possible interactions and temporal/spatial functional specificity for other homeoproteins such as Msx2 and Dlx5 in the transcriptional regulation of Dspp. Dlx3 is most likely acting in concert with other factors to modulate the transcription of target genes. Furthermore, Dlx3 is highly expressed in tissues like the calvaria where Dspp expression is absent or minimal (data not shown). Therefore, the specificity of Dlx3 transcriptional activity in different tissues must be related to its interaction with distinct transactivation partners defining the regulation of tissue-specific target proteins. These tissue-specific partners remain to be identified. However, we show here that the deletion of Dlx3 alone is enough to significantly down-regulate the expression of Dspp in odontoblasts.

Interestingly, Dspp and Dmp1 knock-out mice exhibit a similar tooth phenotype and Dspp expression was shown to be regulated by Dmp1, another non-collagenous matrix protein abundantly expressed in dentin and bone (47, 48). In our model, the knock-out of Dlx3 results in a significant decrease in Dspp expression, without affecting Dmp1. This demonstrates that the presence of Dmp1 in odontoblasts is not sufficient to maintain Dspp expression. Moreover, the fact that Dmp1 expression is not affected in Wnt1-cre:Dlx3$^{F/LacZ}$ mice further supports the specificity of Dspp regulation by Dlx3, and demonstrates that the decrease in Dspp expression does not reflect a general impairment of odontoblast differentiation.

Despite the early and widespread expression of Dlx3 in the dental mesenchyme, the defects observed in the Wnt1-cre:Dlx3$^{F/LacZ}$ mice account for relatively late alterations in cytodifferentiation of odontoblasts, at least for molars. The absence of dentin on the most lingual aspect of mandibular incisors in Wnt1-cre:Dlx3$^{F/LacZ}$ mice suggest an early effect of the NC deletion of Dlx3, specifically on this continuously growing incisor. Previous studies have suggested that the root-analog side of the incisor is a structural entity (49, 50). Interestingly, maxillary incisors are not affected in the same way. The presence of the lingual cervical loop suggests that the progression of the dental epithelium on the lingual side of the tooth is not affected. The absence of dentin production in this area might be due to a disruption in the interactions between epithelial cells and odontoblasts, a change in the fate of the subpopulation of neural crest cells migrating to this area, or a defect in the migration of these cells during early development. These hypotheses remain to be tested.

Tooth development involves crucial interactions between the dental mesenchyme and the dental epithelium through the extracellular matrix (51), and changes in dentin composition can potentially affect ameloblast differentiation (32). In our model, no visible defects in ameloblast differentiation and enamel formation were detected. This observation suggests that, even though the absence of Dlx3 affects dentin maturation, the dentin matrix components required for the initial inductive signals to the dental epithelium are still produced by odontoblasts lacking Dlx3. However, a decrease in Mmp20, Klk4, and Enamelin expression was determined in the mandibles of Wnt1cre:Dlx3$^{F/LacZ}$ mice. Mice that are null for any of these markers exhibit profound enamel defects (36–38). Although they are primarily known for their role in enamel maturation, Mmp20 and Klk4 are also known to be expressed in the dental mesenchyme (39). Given the absence of enamel defects observed in Wnt1cre:Dlx3$^{F/LacZ}$ mice, it is likely that the decrease observed for these markers primarily reflects a decrease in the mesenchymal compartment of the tooth.

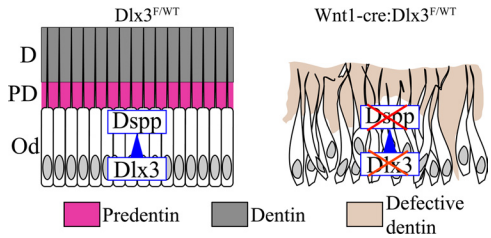

FIGURE 8. **Effects of NC deletion of Dlx3 on tooth development.** Schematic representation of the effects of NC deletion of Dlx3 on odontoblast differentiation, Dspp expression and dentin deposition/mineralization. *D*, dentin; *PD*, predentin: *Od*, odontoblasts.

By targeting the deletion of Dlx3 to the NC, we investigated the function of Dlx3 in tooth development and identified Dspp as a major Dlx3 target in dentin development (Fig. 8). The elucidation of this pathway is a major step in the understanding of the normal function of Dlx3 in tooth development.

Acknowledgments—We thank Dr. Larry W. Fisher for providing us with Dspp riboprobe and anti-Dsp antibody. For the use of instruments, we thank Dr. Richard Leapman (Scanning Electron Microscopy) and Dr. Pamela G. Robey (X-ray). For microarray analysis, we thank George Poy and Weiping Chen. We thank the Mouse Imaging Facility of the National Institutes of Health and the Light Imaging Section of the NIAMS.

REFERENCES

1. Price, J. A., Bowden, D. W., Wright, J. T., Pettenati, M. J., and Hart, T. C. (1998) Identification of a mutation in DLX3 associated with tricho-dento-osseous (TDO) syndrome. *Hum. Mol. Genet.* **7,** 563–569
2. Nieminen, P., Lukinmaa, P. L., Alapulli, H., Methuen, M., Suojärvi, T., Kivirikko, S., Peltola, J., Asikainen, M., and Alaluusua, S. (2011) DLX3 homeodomain mutations cause tricho-dento-osseous syndrome with novel phenotypes. *Cells Tissues Organs* **194,** 49–59
3. Dong, J., Amor, D., Aldred, M. J., Gu, T., Escamilla, M., and MacDougall, M. (2005) DLX3 mutation associated with autosomal dominant amelogenesis imperfecta with taurodontism. *Am. J. Med. Genet.* 133, 138–141
4. Lee, S. K., Lee, Z. H., Lee, S. J., Ahn, B. D., Kim, Y. J., Lee, S. H., and Kim, J. W. (2008) DLX3 mutation in a new family and its phenotypic variations. *J. Dent. Res.* **87,** 354–357
5. Wright, J. T., Hong, S. P., Simmons, D., Daly, B., Uebelhart, D., and Luder, H. U. (2008) DLX3 c.561_562delCT mutation causes attenuated phenotype of tricho-dento-osseous syndrome. *Am. J. Med. Genet. A* **146,** 343–349
6. Mayer, D. E., Baal, C., Litschauer-Poursadrollah, M., Hemmer, W., and Jarisch, R. (2010) Uncombable hair and atopic dermatitis in a case of trichodento-osseous syndrome. *J. Dtsch. Dermatol. Ges.* **8,** 102–104
7. Choi, S. J., Roodman, G. D., Feng, J. Q., Song, I. S., Amin, K., Hart, P. S., Wright, J. T., Haruyama, N., and Hart, T. C. (2009) *In vivo* impact of a 4 bp deletion mutation in the DLX3 gene on bone development. *Dev. Biol.* **325,** 129–137
8. Choi, S. J., Song, I. S., Feng, J. Q., Gao, T., Haruyama, N., Gautam, P., Robey, P. G., and Hart, T. C. (2010) Mutant DLX 3 disrupts odontoblast

polarization and dentin formation. *Dev. Biol.* **344,** 682–692
9. Morasso, M. I., Grinberg, A., Robinson, G., Sargent, T. D., and Mahon, K. A. (1999) Placental failure in mice lacking the homeobox gene Dlx3. *Proc. Natl. Acad. Sci. U.S.A.* **96,** 162–167
10. Hwang, J., Mehrani, T., Millar, S. E., and Morasso, M. I. (2008) Dlx3 is a crucial regulator of hair follicle differentiation and cycling. *Development.* **135,** 3149–3159
11. Hwang, J., Kita, R., Kwon, H. S., Choi, E. H., Lee, S. H., Udey, M. C., and Morasso, M. I. (2011) Epidermal ablation of Dlx3 is linked to IL-17-associated skin inflammation. *Proc. Natl. Acad. Sci. U.S.A.* **108,** 11566–11571
12. Hassan, M. Q., Javed, A., Morasso, M. I., Karlin, J., Montecino, M., van Wijnen, A. J., Stein, G. S., Stein, J. L., and Lian, J. B. (2004) *Mol. Cell. Biol.* **24,** 9248–9261
13. Hassan, M. Q., Tare, R. S., Lee, S. H., Mandeville, M., Morasso, M. I., Javed, A., van Wijnen, A. J., Stein, J. L., Stein, G. S., and Lian, J. B. (2006) BMP2 commitment to the osteogenic lineage involves activation of Runx2 by DLX3 and a homeodomain transcriptional network. *J. Biol. Chem.* **281,** 40515–40526
14. Robinson, G. W., and Mahon, K. A. (1994) Differential and overlapping expression domains of Dlx-2 and Dlx-3 suggest distinct roles for Distal-less homeobox genes in craniofacial development. *Mech. Dev.* **48,** 199–215
15. Chai, Y., Jiang, X., Ito, Y., Bringas, P., Jr., Han, J., Rowitch, D. H., Soriano, P., McMahon, A. P., and Sucov, H. M. (2000) Fate of the mammalian cranial neural crest during tooth and mandibular morphogenesis. *Development* **127,** 1671–1679
16. Zhao, Z., Stock, D., Buchanan, A., and Weiss, K. (2000) Expression of Dlx genes during the development of the murine dentition. *Dev. Genes Evol.* **210,** 270–275
17. Depew, M. J., Simpson, C. A., Morasso, M., and Rubenstein, J. L. (2005) Reassessing the Dlx code: the genetic regulation of branchial arch skeletal pattern and development. *J. Anatomy* **207,** 501–561
18. McGuinness, T., Porteus, M. H., Smiga, S., Bulfone, A., Kingsley, C., Qiu, M., Liu, J. K., Long, J. E., Xu, D., and Rubenstein, J. L. (1996) Sequence, organization, and transcription of the Dlx-1 and Dlx-2 locus. *Genomics* **35,** 473–485
19. Nakamura, S., Stock, D. W., Wydner, K. L., Bollekens, J. A., Takeshita, K., Nagai, B. M., Chiba, S., Kitamura, T., Freeland, T. M., Zhao, Z., Minowada, J., Lawrence, J. B., Weiss, K. M., and Ruddle, F. H. (1996) Genomic analysis of a new mammalian distal-less gene: Dlx7. *Genomics* **38,** 314–324
20. Qiu, M., Bulfone, A., Ghattas, I., Meneses, J. J., Christensen, L., Sharpe, P. T., Presley, R., Pedersen, R. A., and Rubenstein, J. L. (1997) Role of the Dlx homeobox genes in proximodistal patterning of the branchial arches: mutations of Dlx-1, Dlx-2, and Dlx-1 and -2 alter morphogenesis of proximal skeletal and soft tissue structures derived from the first and second arches. *Dev. Biol.* **185,** 165–184
21. Thomas, B. L., Tucker, A. S., Qui, M., Ferguson, C. A., Hardcastle, Z., Rubenstein, J. L., and Sharpe, P. T. (1997) Role of Dlx-1 and Dlx-2 genes in patterning of the murine dentition. *Development* **124,** 4811–4818
22. Lézot, F., Thomas, B., Greene, S. R., Hotton, D., Yuan, Z. A., Castaneda, B., Bolaños, A., Depew, M., Sharpe, P., Gibson, C. W., and Berdal, A. (2008) Physiological implications of DLX homeoproteins in enamel formation. *J. Cell Physiol.* **216,** 688–697
23. Danielian, P. S., Muccino, D., Rowitch, D. H., Michael, S. K., and McMahon, A. P. (1998) Modification of gene activity in mouse embryos in utero by a tamoxifen-inducible form of Cre recombinase. *Curr. Biol.* **8,** 1323–1326
24. Yadav, H., Quijano, C., Kamaraju, A. K., Gavrilova, O., Malek, R., Chen, W., Zerfas, P., Zhigang, D., Wright, E. C., Stuelten, C., Sun, P., Lonning, S., Skarulis, M., Sumner, A. E., Finkel, T., and Rane, S. G. (2011) Protection from obesity and diabetes by blockade of TGF-β/Smad3 signaling. *Cell Metab.* **14,** 67–79
25. Morasso, M. I. (2010) Detection of gene expression in embryonic tissues and stratified epidermis by in situ hybridization. *Methods Mol. Biol.* 585, 253–260
26. Ogbureke, K. U., and Fisher, L. W. (2004) Expression of SIBLINGs and their partner MMPs in salivary glands. *J. Dent. Res.* **83,** 664–670
27. Lee, T. I., Johnstone, S. E., and Young, R. A. (2006) Chromatin immunoprecipitation and microarray-based analysis of protein location. *Nat. Protoc.* **1,** 729–748
28. Langmead, B., Trapnell, C., Pop, M., and Salzberg, S. L. (2009) Ultrafast and memory-efficient alignment of short DNA sequences to the human genome. *Genome Biol.* 10, R25
29. Ji, H., Jiang, H., Ma, W., Johnson, D. S., Myers, R. M., and Wong, W. H. (2008) An integrated software system for analyzing ChIP-chip and ChIP-seq data. *Nat. Biotechnol.* **26,** 1293–1300
30. Zang, C., Schones, D. E., Zeng, C., Cui, K., Zhao, K., and Peng, W. (2009) A clustering approach for identification of enriched domains from histone modification ChIP-Seq data. *Bioinformatics* **25,** 1952–1958
31. Duverger, O., Lee, D., Hassan, M. Q., Chen, S. X., Jaisser, F., Lian, J. B., and Morasso, M. I. (2008) Molecular consequences of a frameshifted DLX3 mutant leading to Tricho-Dento-Osseous syndrome. *J. Biol. Chem.* **283,** 20198–20208
32. He, P., Zhang, Y., Kim, S. O., Radlanski, R. J., Butcher, K., Schneider, R. A., and DenBesten, P. K. (2010) Ameloblast differentiation in the human developing tooth: effects of extracellular matrices. *Matrix Biol.* **29,** 411–419
33. Kim, J. W., Hu, J. C., Lee, J. I., Moon, S. K., Kim, Y. J., Jang, K. T., Lee, S. H., Kim, C. C., Hahn, S. H., and Simmer, J. P. (2005) Mutational hot spot in the DSPP gene causing dentinogenesis imperfecta type II. *Hum. Genet.* **116,** 186–191
34. Sreenath, T., Thyagarajan, T., Hall, B., Longenecker, G., D'Souza, R., Hong, S., Wright, J. T., MacDougall, M., Sauk, J., and Kulkarni, A. B. (2003) Dentin sialophosphoprotein knockout mouse teeth display widened predentin zone and develop defective dentin mineralization similar to human dentinogenesis imperfecta type III. *J. Biol. Chem.* **278,** 24874–24880
35. Yamakoshi, Y., Hu, J. C., Iwata, T., Kobayashi, K., Fukae, M., and Simmer, J. P. (2006) Dentin sialophosphoprotein is processed by MMP-2 and MMP-20 *in vitro* and *in vivo*. *J. Biol. Chem.* **281,** 38235–38243
36. Bartlett, J. D., Beniash, E., Lee, D. H., and Smith, C. E. (2004) Decreased mineral content in MMP-20-null mouse enamel is prominent during the maturation stage. *J. Dent. Res.* **83,** 909–913
37. Simmer, J. P., Hu, Y., Lertlam, R., Yamakoshi, Y., and Hu, J. C. (2009) Hypomaturation enamel defects in Klk4 knockout/LacZ knockin mice. *J. Biol. Chem.* **284,** 19110–19121
38. Hu, J. C., Hu, Y., Smith, C. E., McKee, M. D., Wright, J. T., Yamakoshi, Y., Papagerakis, P., Hunter, G. K., Feng, J. Q., Yamakoshi, F., and Simmer, J. P. (2008) Enamel defects and ameloblast-specific expression in Enam knockout/lacz knock-in mice. *J. Biol. Chem.* **283,** 10858–10871
39. Hu, J. C., Sun, X., Zhang, C., Liu, S., Bartlett, J. D., and Simmer, J. P. (2002) Enamelysin and kallikrein-4 mRNA expression in developing mouse molars. *Eur. J. Oral. Sci.* 110, 307–315
40. Laajala, T. D., Raghav, S., Tuomela, S., Lahesmaa, R., Aittokallio, T., and Elo, L. L. (2009) A practical comparison of methods for detecting transcription factor binding sites in ChIP-seq experiments. *BMC Genomics* **10,** 618
41. Feledy, J. A., Morasso, M. I., Jang, S. I., and Sargent, T. D. (1999) Transcriptional activation by the homeodomain protein distal-less 3. *Nucleic Acids Res.* **27,** 764–770
42. Duverger, O., Chen, S. X., Lee, D., Li, T., Chock, P. B., and Morasso, M. I. (2011) SUMOylation of DLX3 by SUMO1 promotes its transcriptional activity. *J. Cell Biochem.* **112,** 445–452
43. Feng, J. Q., Luan, X., Wallace, J., Jing, D., Ohshima, T., Kulkarni, A. B., D'Souza, R. N., Kozak, C. A., and MacDougall, M. (1998) Genomic organization, chromosomal mapping, and promoter analysis of the mouse dentin sialophosphoprotein (Dspp) gene, which codes for both dentin sialoprotein and dentin phosphoprotein. *J. Biol. Chem.* **273,** 9457–9464
44. Chen, S., Unterbrink, A., Kadapakkam, S., Dong, J., Gu, T. T., Dickson, J., Chuang, H. H., and MacDougall, M. (2004) Regulation of the cell type-specific dentin sialophosphoprotein gene expression in mouse odontoblasts by a novel transcription repressor and an activator CCAAT-binding factor. *J. Biol. Chem.* **279,** 42182–42191
45. Chen, S., Gluhak-Heinrich, J., Martinez, M., Li, T., Wu, Y., Chuang, H. H., Chen, L., Dong, J., Gay, I., and MacDougall, M. (2008) Bone morphogenetic protein 2 mediates dentin sialophosphoprotein expression and odontoblast differentiation via NF-Y signaling. *J. Biol. Chem.* **283,** 19359–19370

46. Cho, Y. D., Yoon, W. J., Woo, K. M., Baek, J. H., Park, J. C., and Ryoo, H. M. (2010) The canonical BMP signaling pathway plays a crucial part in stimulation of dentin sialophosphoprotein expression by BMP-2. *J. Biol. Chem.* **285,** 36369–36376
47. Ye, L., MacDougall, M., Zhang, S., Xie, Y., Zhang, J., Li, Z., Lu, Y., Mishina, Y., and Feng, J. Q. (2004) Deletion of dentin matrix protein-1 leads to a partial failure of maturation of predentin into dentin, hypomineralization, and expanded cavities of pulp and root canal during postnatal tooth development. *J. Biol. Chem.* **279,** 19141–19148
48. Narayanan, K., Gajjeraman, S., Ramachandran, A., Hao, J., and George, A. (2006) Dentin matrix protein 1 regulates dentin sialophosphoprotein gene transcription during early odontoblast differentiation. *J. Biol. Chem.* **281,** 19064–19071
49. Opsahl, S., Septier, D., Aubin, I., Guenet, J. L., Sreenath, T., Kulkarni, A., Vermelin, L., and Goldberg, M. (2005) Is the lingual forming part of the incisor a structural entity? Evidences from the fragilitas ossium (fro/fro) mouse mutation and the TGFβ1-overexpressing transgenic strain. *Arch. Oral. Biol.* **50,** 279–286
50. Park, J. C., Herr, Y., Kim, H. J., Gronostajski, R. M., and Cho, M. I. (2007) Nfic gene disruption inhibits differentiation of odontoblasts responsible for root formation and results in formation of short and abnormal roots in mice. *J. Periodontol* **78,** 1795–1802
51. Thesleff, I. (2006) The genetic basis of tooth development and dental defects. *Am. J. Med. Genet A* **140,** 2530–2535